

## REMARKS

Claims 1-5, 8 and 9 are currently active.

The Examiner requests the reference to the prior application be inserted as the first sentence of the specification of the subject application or in an application data sheet. Respectfully, it is pointed out to the Examiner that on page 2 of 5 of the transmittal, applicants already request a reference be inserted in the specification to the prior application.

Applicants are reviewing the drawings and are considering changes to the drawings in regard to reference numbers and labels and descriptions for graphs or plots and corresponding features of curves. Formal drawings will be submitted when the application is allowed. A substitute figure 1 is enclosed herewith that has reference labels added, as shown in red, no new matter has been added.

Claims 6 and 7 have been deleted.

The Examiner has rejected claims 1-9 under 35 U.S.C. 112, second paragraph. Claims 1-9 have been amended to obviate this rejection.

The Examiner has objected to the disclosure for various informalities. The application has been amended to obviate this rejection.

The Examiner has rejected Claims 1-4, 6, 8 and 9 as being anticipated by Hamilton. The Examiner has rejected Claim 9 as being anticipated by Van Gorkom. The Examiner has rejected Claims 5 and 7 as being unpatentable below over Hamilton. Applicants respectfully traverse this rejection in light of the amendments to the claims. The claims, as amended, have the limitation of a resulting gain of electronics.

The applied art record does not teach or suggest this limitation. Accordingly, Claims 1-5, 8 and 9 are patentable over the applied art record.

In view of the foregoing amendments and remarks, it is respectfully requested that the outstanding rejections and objections to this application be reconsidered and withdrawn, and Claims 1-5, 8 and 9, now in this application be allowed.

**CERTIFICATE OF MAILING**

I hereby certify that the correspondence is being deposited with the United States Postal Service as first class mail in an envelope addressed to Assistant Commissioner for Patents, Washington, D.C. 20581.

on 2/11/03  
Ansel M. Schwartz  
Ansel M. Schwartz  
Registration No. 30,587  
2/11/03  
Date

Respectfully submitted,

FREDERICK MICHAEL MAKO, ET AL.

By Ansel Schwartz

Ansel M. Schwartz, Esquire  
Reg. No. 30,587  
One Sterling Plaza  
201 N. Craig Street  
Suite 304  
Pittsburgh, PA 15213  
(412) 621-9222

Attorney for Applicant

**Version with markings to show changes made to the specification :**

Page 2, lines 1-9:

With this relatively complex system, Boeing obtains a peak current up to about 400 A in pulses of 15 to 20 ps duration, with good emittance. The bunching process yields a peak current which is two orders of magnitude larger than the electron gun current. Space charge forces, which cause the beam to expand both radially and axially, are minimized by using a strong electric field in the high-power buncher, and finally are balanced by forces due to the axial magnetic field. The performance achieved by Boeing appears to be at or near the limit of this type of injector.

Page 8, lines 21-23:

Figure 30 is a schematic drawing of a set of electrode shapes for a high-power diode using the modified formulas to the usual Pierce shapes as discussed [in the text] below.

Page 11, line 27 through page13, line 4:

A schematic of one embodiment of the proposed device is given in Fig. 2. Although the design shown is not necessarily optimum it provides a basis for describing the

invention. Shown in Fig. 2 is a side view of a cylindrically symmetric device. [Rf] The rf power is fed into the cavity by a low impedance coaxial transmission line connected to the perimeter of the cavity. Alternatively, rf power may be fed into the cavity by the conventional method of side coupling using a tapered waveguide. The appropriate mode is then set up (in this case the  $TM_{020}$  mode). An annular electron pulse is generated by secondary emission at the second peak of the electric field in the cavity operating in a  $TM_{020}$  mode. The first peak is eliminated by placing an inner conducting cylinder at the first zero of the  $TM_{020}$  mode. The pulse rapidly bunches and reaches a saturated state within several rf periods. This rapid bunching and saturation is due to a combination of the space charge field and the resonant rf field condition. The right wall of the cavity in Fig. 2 (also see detail) is constructed with a transmitting annular shaped double screen (grid) which allows for the transmission of a high current density hollow electron pulse. The radial wires maintain a path for the rf current. The double screen provides a means to isolate the accelerating and rf fields thus preventing the accelerating field from pulling out electrons that are not resonant with the rf field. Also, the second grid (to the right) is electrically isolated from the first grid and can be dc biased (  $\approx -$  100 volts) to create a barrier for low energy electrons. The emittance in the micro-pulse gun (MPG) is lower than would be expected for a dc gun. The main point is that the resonant particles are loaded into the wave at low phase angles and when they reach the opposite electrode or grid, they experience a reduced transverse kick from the grid wires. Inside the

cavity, radial expansion is controlled by an axial magnetic field. The short-pulse, high-current electron pulse leaves the cavity with high kinetic energy. The pulse is then accelerated to much higher energy by either electrostatic, inductive or rf means. The application for the above hollow beam configuration is primarily suited to high harmonic microwave production. An alternative configuration which produces a solid beam is the  $TM_{010}$  mode. This configuration will be more suitable for injector applications.

Page 36, lines 4-23:

In Fig. 17, the "resonant tuning curve" is plotted for the micro-pulse electron gun from the PIC simulations and the theoretical prediction. The importance of this plot is the fact that it describes the "tolerance" of the MPG to deviations in cavity voltage, gap spacing, or frequency, and it indicates the striking agreement between theory and PIC simulation. For simulations with a cavity gap length  $d = 0.5$  cm the peak current density is plotted for various frequencies as a function of the normalized rf field  $\alpha_0$ . Figure 17 suggests that the MPG has a high tolerance, and that errors in the field or gap spacing can be easily accommodated in the resonance process. For instance, as is seen from Table 3 at a frequency of 1.3 GHz, the current density  $J_x$  at an applied voltage of 2.4 kV is an order of magnitude less than it is at 4.3 kV. However,  $J_x$  climbs rapidly from this value as the voltage approaches 6.4 kV, and then turns over and goes to zero again at 9.8 kV. Also displayed in Fig. 17 is the theoretical

tuning curve obtained from the equations above [in Section 3.5.1]. As can be seen, the agreement between theory and the two-dimensional PIC simulations is excellent. At high  $\alpha_0$  such that  $\alpha_0 > 0.6$  the analytic theory is suspect since it does not include relativistic effects.

Page 38, lines 20-25:

In Fig. 22, the same electric field is shown for the above cavity except a 1 cm diameter, 40 amp/cm<sup>2</sup>, 25 ps long beam is emitted into the cavity. The space charge of the beam decreases the driving electric field by about 1/3. This beam loading, as discussed previously with regard to the tuning curve, does not significantly alter the resonance.

Page 41, lines 3-16:

The accelerating field (after the cavity and second grid) produces a transverse kick as the electrons pass the second grid. However, this field is substantially reduced when we introduce an electrode which makes an angle of 45 ° with the beam exiting the grid. Only the bottom of this 45 ° electrode is shown in Fig. 27. The introduction of this electrode is to focus the micro-pulse [(see Section 3.10)]; the angle of 45 ° is optional for high energy electrons [W. Peter, Journal of Applied Physics 71, 3197 (1992)]. For emission, this angle becomes  $3\pi/8$ , that is, the Pierce angle. The fact that this 45 ° electrode will reduce the

transverse fields by an order of magnitude is a fortunate outcome of our studies. This also allows for higher gradients outside the cavity. Thus, the kick from the second grid does not significantly affect the emittance.

Page 42, lines 1-12:

Figure 28 shows the emittance and transmission results using an ac voltage. The normalized emittance starts at zero and grows to 2.5 mm-mrad just before the first grid. The emittance after both grids decreases as the number of grid wires per 5 mm radial extent increases. With reasonable transmission (52%), an emittance within a factor of two of its value before the grid can be obtained. If "rms addition" is applied to the secondary source emittance of 7 mm-mrad [(Sect. 3.4.1)] and to those on Fig. 28 a range of 9-18 mm-mrad as the final extracted beam emittance is obtained. For the given space charge, the best emittance to charge ratio of 3 mm-mrad/nC is obtained, including all sources of emittance for the extracted beam.

Page 48, lines 1-8:

For the above sample parameters, a 16% expansion occurs. Equation (47) also underestimates the expansion for the same reasons as above so again a numerical integration of the equation of motion was performed. The results show that a 44% expansion of the bunch

length occurs, however, the pulse width decreases from 5 psec to about 3.5 psec. These results do not have a significant impact on the performance of the device, as demonstrated in the computer simulations.

Page 48, lines 23 and 24:

where  $\lambda \equiv (2e/m)^{1/4} / (9\pi J)^{1/2}$ . Integrating this expression gives  $\phi(x)$  as a function of  $x$  in terms of the following cubic equation

Page 56, lines 8-27:

For a typical injector application, a finite magnetic field at the emitting surface in the MPG is not used because it would impair the emittance downstream. For this reason, an alternative to magnetic focusing within the MPG is proposed, namely to shape the cavity of the MPG so it employs moderate electrostatic focusing. As described above [in Section 3.10], classical Pierce shaping cannot be directly used in the present situation since the micropulse from the emitter (Fig. 46) is not space-charge limited. In this case, the appropriate electrode shaping can be solved for from the theory presented above [in Section 3.10]. Note that this focusing is essentially "one-way", i.e., the micropulse emitted off the exit grid which returns to the emitting surface  $S$  will be slightly *de-focused* during its transit. However, a slightly de-focused returning pulse can be tolerated since its only *raison d'etre* is to provide a source of



electrons for creation of anew batch of secondary electrons off the surface S. Hence, the only possible disadvantage of a de-focused returning micropulse would be to cause some secondary electrons to strike the opposite wall of the cavity outside of S and thus to represent a possible decrease in the cavity  $Q$ .

Version with markings to show changes made to the claims

1. An electron gun comprising:

an RF cavity having a first side with an emitting surface and a second side with a transmitting and emitting section; and

a mechanism for producing an oscillating force which encompasses the emitting surface and the section so electrons are directed between the emitting surface and the transmitting and emitting section to contact the emitting surface and generate additional electrons and to contact the transmitting and emitting section to generate additional electrons or escape the cavity through the transmitting and emitting section, with a resulting gain of electrons in a unidirectional flow after  $N_{RF}$  periods is  $[\delta_2 \delta_1 (1-T)]^N$ , where N is an integer greater than or equal to one,  $\delta_1$ , is the number of secondary electrons emitted from the emitting surface, T is the ratio of transmitted to incident electrons for the section, and  $\delta_2$  is the section electron secondary yield.

2. A gun as described in Claim 1 wherein said transmitting and emitting section isolating the cavity from external forces [on outside] to the cavity [and adjacent].

3. A gun as described in Claim 2 wherein the transmitting and emitting section includes a transmitting and emitting double screen.

4. A gun as described in Claim 3 wherein the producing mechanism includes a mechanism for producing an oscillating electric field disposed adjacent the RF cavity that provides the force and [which] has a radial component that confines the electrons to [the] a region between the respective double screen and the corresponding emitting surface.

5. A gun as described in Claim 4 wherein the respective double screen is of an annular shape.

8. A gun as described in Claim 4 including a mechanism for producing a magnetic field disposed adjacent the RF cavity to force the electrons to stay between the respective double screen and the corresponding emitting surface.

9. A method for producing electrons characterized by the steps of:

moving at least a first electron in a first direction;

striking a first area with the first electron;

producing additional electrons at the first area due to the first electron;

moving the additional electrons from the first area to a second area; and

transmitting the additional electrons through the second area and creating [more]

$\delta_2[\delta_1(1-T)]$  secondary electrons due to the additional electrons from the first area striking the second area, where  $N$  is an integer greater than or equal to one,  $\delta_1$  is the number of secondary electrons emitted from the emitting surface,  $T$  is the ratio of transmitted to incident electrons for the section, and  $\delta_2$  is the section electron secondary yield.

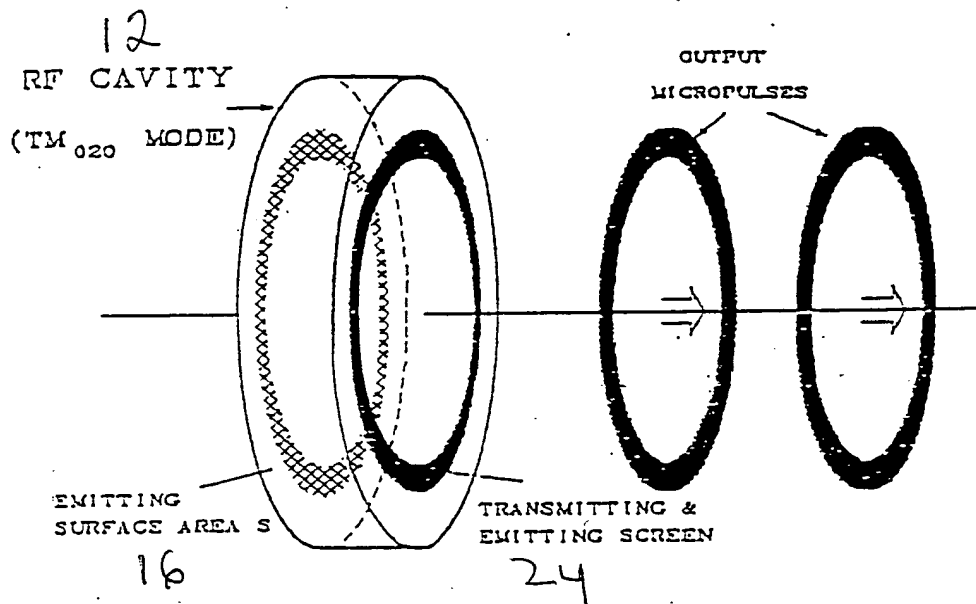


Figure 1: Perspective view of the micropulse gun for a hollow beam in the  $TM_{020}$  mode. The inner conductor is not shown.